

Sandia National Laboratories
University Alliance Design Competition 2010
Texas Tech University - Novel Design Entry



MICROBOTIC
CHESS PLAYER

I. Abstract

This white paper describes the design of a *Microbotic Chess Player* system developed using the SUMMiT V fabrication process. This design consists of the *World's Smallest Chess Set* and is capable of being played using on-chip robotic manipulator. A 2-DOF microrobotic arm is driven by long travel actuators. In addition to furthering research in the area of micromanipulation, this chess player could prove to be fascinating for chess playing students over a range of education levels. The long-travel, bi-directional linear actuator is designed to have total travel of 405 μm with a minimum step size of 9 μm . A series of experimental procedures are proposed for complete characterization and testing the functionality of the fabricated system.

II. Objective

The objective is to produce a playable micro-Chess game by:

- Designing a checkerboard having chess pieces capable of being maneuvered using an *on-chip* 2-axis manipulator.
- Developing a 2-axis positioning system.
- Developing a bi-directional long travel actuator capable of hovering over the entire span of the chess board.

III. Introduction

In Microelectromechanical Systems (MEMS), micro- and nanometer-sized object manipulation has found importance and applications in many areas. For instance, manipulation of carbon nanotubes and nano-particles using atomic force microscope (AFM) [1, 2] and getting the visual feedback while in a scanning electron microscope (SEM) or transmission electron microscope (TEM) [3,4,5] has been demonstrated. Microassembly is necessary for sub-centimeter-scale microsystems that incorporate solid-state light sources such as LEDs or lasers into MEMS optical applications. The development of linear actuators has made possible MEMS devices for micro/nano positioning, biological cell probing, medical devices and micro-scale optical systems. There are always tradeoffs between minimum and maximum displacement, force, and degrees of freedom to be considered when designing such systems. Thermal actuators have proven to be a robust actuation method in surface micromachined MEMS. They generate a relatively large output force and sufficient displacement at low actuation voltages, which make them an attractive alternative to more traditional electrostatic actuation methods.

In an attempt to develop synergy between the Texas Tech University (TTU) MEMS group and other academic institutes on campus, we initiated contact with TTU's Susan Polgar Institute for Chess Excellence (SPICE). Grand Master Susan Polgar, is one of the top chess players in the world, and heads this institute. Chess, which has its origins in the 7th century, is an international game that is widely played across nearly all age groups. Using the game of chess, we will demonstrate the capability of a novel, 2-axis micro-manipulator for moving and positioning microstructures. In addition to being an important advancement in on-chip manipulators, the system will be the nexus for educational endeavors, by engaging students at all levels. This manipulator is designed to produce long travel (100's of microns) in small step sizes (~10 microns) with minimum power requirements, i.e. zero power latching. The design will be fabricated using the Sandia Ultra-planer, Multi-level MEMS Technology 5 (SUMMiT VTM) process. Exploiting the strengths of this five-layer process, we designed the chess board, pieces,

and the manipulator to move the pieces over the whole span of the chess board. The manipulator is comprised of a bi-directional, two-axis MEMS positioning system and bi-directional actuators.

IV. Description

Device Design

The AutoCAD design for the *Microbotic Chess Player* is shown in Figure 1. The system can be broken down into three key components: (1) chess board and pieces, (2) two-axis MEMS positioning system, for enabling 2-DOF motion and (3), and two, long travel bi-directional linear ratcheting actuators.

Chess Board and Pieces

The chess board (Figure 2) is an eight-by-eight grid with total dimensions of 435 μ m x 435 μ m. The colors of the sixty-four squares alternate and are made using the patterned and un-patterned *Poly0* layer for making "light squares" and "dark squares," respectively. The chess board has sixteen chess pieces on each side. Each piece has its shape in the *Poly2* layer with a *Poly3* layer stub attached to it. This stub acts as an end-effector handling area, where the manipulator end will interface with the chess piece. Figure 4 shows the 3-D model and a cross-section view of a chess piece. After the sacrificial oxide release, the pieces will still be attached to the substrate through a 1 μ m diameter *Poly1* via connected to *Poly0*. This via is just enough to hold the piece in-place, post-release.

The end-effector (Figure 5) has a circular area which is held over the board using a *Poly4* cantilever and comes into contact with the *Poly3* stub on each chess piece, as shown in Figure 6. The end-effector is provided with small semicircular protrusions which will minimize contact area and reduce stiction. An external path has been provided along each side of the chess board which allows movement of chess pieces without having to jump other pieces. This path has a boundary formed using *Poly2* which acts as a stop and doesn't allow chess pieces to exit the board. The dimensions of the path are such that 15 knocked-off micro-chess pieces can be placed outside the area of the chess board.

Figures 7 and 8 show the SEM images of a chess board and pieces fabricated on the 2009 Texas Tech University (TTU) Sandia design competition chip. The board was 1 mm x 1mm square with 100 μ m diameter pieces. This version was designed for being played using an off-chip microgripper capable of being operated in 3-dimensions with micron scale control. A sharp probe or a microgripper can be used to pick and place the chess pieces. The present version is designed to be played using the on-chip manipulator. The area of the chess board and the pieces have been scaled down by a factor of 2 (in both X and Y), compared to the previous version, to lessen the travel required of the manipulator.

Bi-directional Two-Axis MEMS Positioning System

The positioning system, as show in Figure 7, consists of two slotted arms for X and Y axis motion on the *Poly1/2* and *Poly3* layers and a central pin that is constrained between the slots on both the axis arms. The *Poly4* layer is used to cap the main pin. A cantilever arm on *Poly4* is used to connect the central pin to the manipulator probe that can be positioned by the actuation of the positioning system. The pin is constrained by the *Poly1/2* layer for the X-axis and by *Poly3* for the Y-axis. For both the X and Y axis, there is a 1- μ m gap on either side of the pin which allows 2- μ m play in the joint in the XY-axes. In this way, the central pin is constrained

between the two orthogonal slots along the X and Y axis positioning arms and is able to slide along either one. The pin structure, as shown in Figure 11, is supported by a dimple which rests over the *Poly0* layer and will slide over it. Figure 10 shows the *Poly4* guide structure which prevents the out-of-plane buckling of the positioning system. At the ends of the X and Y slotted arms, the support structures have been provided which act both as an abutment and a stop.

Long Travel Bi-directional Linear Actuators

The overall actuator design (Figure 13) is comprised of three important components namely, the central shuttle, ratcheting system, and the side guides. The central shuttle is the basic component of the device which is $64\mu\text{m} \times 735\mu\text{m}$ in dimension. It is a free moving structure located beneath the drive actuator and between the two side chevron actuators. It is composed of the *Poly1-Poly2 laminate* and the *Poly3* layer. The *Poly3* and *Poly2* layers are attached using multiple *SacOx3* cuts. The length of this free moving structure ($280\mu\text{m}$ forward and backward) is kept such that it can span the entire length and breadth of the chess board. There are oppositely facing serrated teeth on either side of the shuttle which are used for its movement in the forward and backward directions, when meshed with the ratchet pawls. The teeth have a pitch size of $9\mu\text{m}$, as shown in Figure 15, which defines the step size of the device. The shuttle also has *Poly1*, *Poly2* and *Poly3* cuts of $2\mu\text{m} \times 2\mu\text{m}$ which act like etch release holes, so that the sacrificial material below these layers is completely removed and a free moving structure is obtained. There are dimples beneath the *Poly1* layer obtained using *Dimple1* cuts so that the contact area between the shuttle and *Poly0* layer is minimized, thus reducing surface stiction. The ratcheting system, shown in Figure 14, is an important part of the device which holds all the mechanism for the device operation. It constitutes of the top chevron actuator (Drive Actuator), ratcheting pawls, and the side chevron actuators. The drive actuator is an overhanging structure built at the *Poly4* layer, which allows it to move without any obstruction. It holds the ratchet pawls on either sides of the shuttle, as shown in Figure 15. A *SacOx4* cut enables connection between the *Poly4* layer and *Poly3* layer. Another *SacOx3* cut is made to attach the *Poly3* layer to the *Poly2* layer. The drive actuator is powered using a separate bond pad and a common ground. It is designed to provide enough force and displacement to help in sliding the pawls on the teeth and move the shuttle in both directions depending on the sets of ratchet pawls engaged the shuttle.

The ratchet pawls are compliant structures composed of the *Poly1-Poly2 laminate*. There are two different types of ratchet pawls used on either sides of the shuttle, one anchored to the *Poly0* layer and the other attached to the *Poly4* drive actuator. The pawls attached to the drive actuator are responsible for moving the shuttle while the pawls which are anchored hold the shuttle in place and prevent any unwanted movement of the shuttle. Also, the pawls are mechanically coupled to the side arm actuators using a pin type structure. A typical 2D cross-section of the ratchet pawl is shown in Figure 16(d). It has a rectangular slot in it, which is made using a *Poly2* cut which makes it free to move in the direction of the drive actuator when it is engaged to the shuttle. It can be disengaged when it is not being used (during actuation of the side arm actuators).

The side chevron actuators are constructed using the *Poly1/2 laminate* layer which allows for the thicker chevron arms, thus increasing the *aspect ratio* and minimizing any out of plane motion of the actuator. It has a special U-shaped structure connected to the middle arm which helps in engagement and disengagement of the ratchet pawls. Two bridge type structures on the *Poly3* layer extend from the side chevrons to the ratchet pawl and the coupling between them is

attained using a dimple at the *Poly1* layer. There is a similar system on the other side of the shuttle for engaging and disengaging the pawls on the other sides. Both the side arm actuators have different bond pads for electrical connection, but share a common ground. The shuttle is held in place by four guides; two located at the front, and two at the back as shown in Figure 17. The guide consists of two anchors on both sides of the shuttle, *Poly0-Poly3* layers with the *Poly4* layer connecting these anchors forming a bridge type structure. The function of the guides prevents in-plane, nonlinear movement of the shuttle, and also out-of-plane movement, thus making it more reliable and maintaining proper linear motion. There is a notch made on the shuttle, as shown in Figure 18, such that initial spacing between the shuttle and guide is $1\mu\text{m}$. Once it moves forward or backward by one step, this spacing reduces to $0.25\mu\text{m}$. There are four side stops, two in the front, and two at the back to prevent any non-linear motion of the drive actuator. These help in keeping the drive actuator in position and not getting pulled sideways by the side chevron actuator when engaging and disengaging the pawls. Figure 10 shows the exploded view of the *Poly4* strap.

The working principle of this design is presented in the next section. A detailed discussion about the actuator performance and positioning system is provided in the modeling section of this paper.

SUMMiT V™ Strengths

The SUMMiT V process provides us with a large number of independent *flat* layers developed by chemical mechanical polishing (CMP) required for developing the bi-directional mechanism that includes chevrons on multiple layers of polysilicon, one-above the other. The gap provided by the SUMMiT process is just enough to provide the air-layer required for cooling and hence the high actuation cycles rates of the electrothermal devices. The thicknesses of the layers (esp. *Poly2*) provide enough resistance and thickness to produce the right amount of thermal expansion with necessary compliance in the chevron actuators. This attribute also helps to get the right amount of meshing between the ratchet pawls and shuttle. *Dimples* provided on layers *Poly4*, *Poly3* and *Poly1* help reduce total stiction. This facet of the SUMMiT process helps us to make the movable pin which in-turn allows the construction of a bi-directional positioning system.

Usefulness of Design for Educational Outreach

Educating society in MEMS technologies is very important in driving the creation of future MEMS devices and applications. Device such as the *Chess Manipulator* can act as a platform to spread the concepts of the micro and nano world to many levels of students.

- *Grades 7-12:* To begin the discussion, we will use the chess board with pieces to promote it as the *World's Smallest Chess Board*. Demonstrating our micro-chess system to grade school students will be useful in educating them in size scaling factors, by comparing the micro devices with biological cells or small insects. It provides an amusing way to promote engineering to prospective students. To actually help students *feel* the push-pull movement of the actuators, we will connect the control of the device to a haptic. Haptics utilize tactile feedback to provide mechanical response to the user by scaling the micro/nano forces to macro level. A commercially available gaming haptic will be interfaced with the proposed device. The force feedback will be simulated with each actuation cycle (LabVIEW routine) of the drive chevron giving a feeling of actually

pushing the shuttle forward. A demonstration of a similar system was given at Lubbock's science museum on the occasion of Science Day (Figure 29).

- *College freshman engineers/physicists:* The device can be used to explain basic physics concepts such as thermal expansion, contraction and heat transfer modes by displaying the operation of electrothermal actuators used in the design. The thermal expansion could be determined and the temperature calibration could be done using ANSYS simulations or infrared imaging.
- *Graduate students:* Lab experiments can be designed for demonstration of multi-level chevron actuators. The device could also be used to exhibit the strengths of SUMMiT V process providing good insight into multi-layered structures and surface micromachining (SMM) technology. Performing *on-chip* handling using this device would interest graduate students and help further its potential applications to the fields of biomolecular manipulation and microassembly.

V. Principle of Operation

The operation procedures can be divided into three major categories:

1. Long travel bi-directional linear actuator mechanism
2. 2-DOF positioning system
3. Chess-piece Manipulation

Long Travel Bi-directional Linear Actuator Mechanism

The system is driven by a combination of electrothermal chevron actuators and a ratcheting mechanism. A central shuttle with oppositely facing ratchet teeth helps attain bi-directional motion using two different sets of chevron actuators viz., 1) Side (*Poly2*) chevron actuators, one on each side and 2) Top chevron actuator (*Poly4*), coupled to a counter ratcheting system. The direction of motion of the shuttle depends on which side chevron actuator is powered 'ON', thus engaging or disengaging the ratchet pawls on respective sides. The serrated teeth on both sides of the shuttle and the shapes of the ratcheting pawls are designed such that the right side of the system helps in moving the shuttle in the forward direction, whereas the left sides assists reverse motion.

Figure 19 illustrates the operation sequence of the system for the forward motion of the shuttle. Event (A) shows the initial position of the system at power down. In Event (B) Left Side chevron actuator is powered 'ON', which disengages both the ratchet pawls on that side and the shuttle is free to move in the forward direction. In Event (C) the Top chevron actuator is powered 'ON' which pull backs one of the ratchet pawl on the right, while the second pawl still holds the shuttle thus preventing any backward motion. Also, the shuttle teeth and the pawls are designed such that the pawl slides out and ratchets on to the next tooth. In Event (D) the Top drive actuator is powered 'OFF' which takes the shuttle along with it one step forward due to ratcheting. In this event, the fixed pawl, locking the movement of the shuttle, slides out and ratchets onto the next tooth, thus making sure that at any particular event one of the four pawls holds the shuttle in place. In Event (E) the Left side chevron actuator is powered 'OFF' if no further step motion is required. The whole sequence of operation is for one step increment of the shuttle and needs to be repeated for more displacements.

Similarly, for reverse motion of the shuttle all the sequences are repeated except that the chevron actuator on the right side is powered ‘ON’ which disengages the pawls on that side and allows for reverse motion. This drive mechanism allows for actuation of the shuttle in both directions with only three relatively simple drive signals and a ground. The unit step motion is determined by the stroke of the drive actuator and the separation of the ratchet teeth on the shuttle. This actuator is capable of zero-power latching, that is, the shuttle maintains its position when the power is turned ‘OFF’. The minimal number of drive signals for this actuator is an improvement on other, similar designs [6].

2-DOF Micro-Positioning System

The basic theory of operation of the device is shown in Figure 20. The main pin structure is the part in the positioning assembly that gets moved in the X and Y directions. Figure 20(a) shows the main pin being held between X and Y stage arms. The stage arms are at different layers and allow the sliding of the pin in both directions through the applied force. As shown in Figure 20(b), for motion along the Y-direction, a force (towards top of page) is applied to the horizontal arm. A force to the left is applied to the vertical arm to move in the X-direction (Figure 20(c)). To achieve motion in both directions, simultaneous forces can be applied to both arms as shown in Figure 20(d). The *Poly4* cantilever structure attached to the pin gets its motion when the linear drives are actuated.

Chess-piece Manipulation

After fabrication, the end-effector stands in the center of the chess board. The X and Y linear drives are actuated, as explained in the previous sections, as per the requirements of the players to position the end-effector next to the chess piece. The semicircular bumps come in contact with the *Poly3* stub on the pieces and nudge them so that the *Poly1* via to the *Poly0* level is broken and the pieces are then pushed to the desired location directly (pawns) or via the path around the chess board (pieces along the back rows). The chess board is in *Poly0* so that it forms a base and it is patterned in such a way that the dimple structures can easily cruise without getting caught in the gaps. Figure 21 shows the game being played by the robot.

Measurements

The primary measurements would focus on the motion characterization of the *Chess Manipulation* system. The optical characterization would be done by utilizing the experimental set-up as shown in Figure 22. It will consist of an optical microscope interfaced with a CCD camera and a custom built power supply unit. A LabVIEW VI will be developed to control the power supply unit (COM port interface) and perform the image acquisition using NI Vision. The CCD camera with motion tracking system (LabView routine) will characterize the motion of the linear drives and analyze the position of the drive with time. The tests will evaluate and quantify step size, maximum travel, and repeatability. The technique of Raman spectroscopy could be used to monitor the temperature changes in the electrothermal actuator with the increase in current through it. A similar optical characterization can be performed for the positioning system and quantify the displacements and repeatability in response to the applied voltage/current along both the X and Y axes. Finally, to complete thorough characterization of the stage, we can gauge the amount of crosstalk (displacements in the un-actuated directions due to cross-axis coupling) between the axes.

VI. Modeling

The bi-directional long-travel linear drive was chosen as the primary actuator for this design of the *Microbotic Chess Player* because of its success in prior designs done at TTU in 2008. The characterization of this device was done experimentally and comparing it to the simulation results in ANSYS. [7].

The bent beam actuators are the most important components of the ratcheting mechanism and the one which govern operation. To obtain an understanding of the device physics and operation, the bent actuators were simulated. Complete three-dimensional actuation of the device is modeled using a 10-node coupled field solid element (227) [8]. The model is a coupled-field electrothermal model with conductive heat flow due to the Joule heating and displacements due to the thermal expansion calculated. The geometry of the devices used for modeling is provided in Figure 23. Figure 24 shows the displacement vector sum of the push-pull chevrons on Bi-directional linear actuator. The material properties reported by Baker *et al.* [9] were employed in this model.

The tests were carried to determine the displacement as well number of steps moved by the shuttle for a given number of actuation cycles and to check for occurrence of any double ratcheting events or skipped events. The side chevron actuators were operated at 11V (60mA) and the top chevron actuator was operated at 12V (54mA). The devices were tested for 10 actuation cycles in forward and reverse direction, each for 20 runs. Figure 25 shows the captured microscope images of the device for forward motion at intervals of 5, 10 and 20 events.

Figure 26 shows the actuation data for four devices that were tested both for forward and reverse motion. From the tests that were performed it can be seen that no skipped events occurred during the actuation, although at times there were a few multiple ratcheting events taking place, thus resulting in more than 10 step movements for given 10 actuation cycles. Figures 27 and 28 show the other test results including I-V and displacement-power plots consumption for both drive as well as the side chevron actuators.

VII. Summary

The design of *Microbotic Chess Player* was achieved by integrating three novel MEMS device designs: long travel bi-directional linear drives, a 2-DOF positioning stage, and the *World's Smallest Chess Board*. The 2-axis linear drives were designed to accomplish the requirements of long travel and sufficient step size for ratcheting (405 μ m and 9 μ m respectively) needed for micro-chess piece manipulation with a 2-DOF positioning system. The actuation system is designed to have minimal cross-talk and play between the X and Y axis. Experiments will be conducted to characterize and test the proposed device.

VIII. Appendix A: Figures

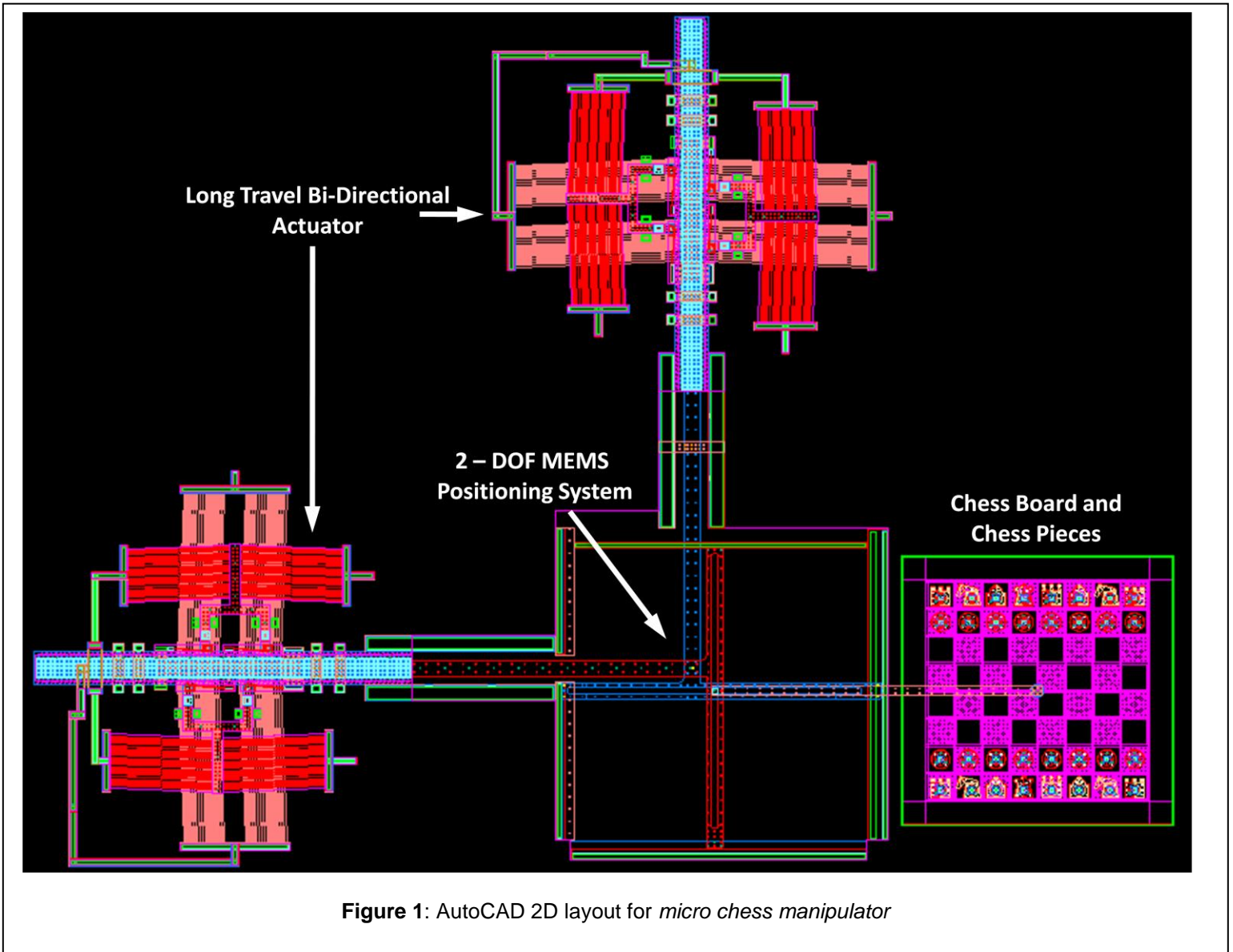


Figure 1: AutoCAD 2D layout for *micro chess manipulator*

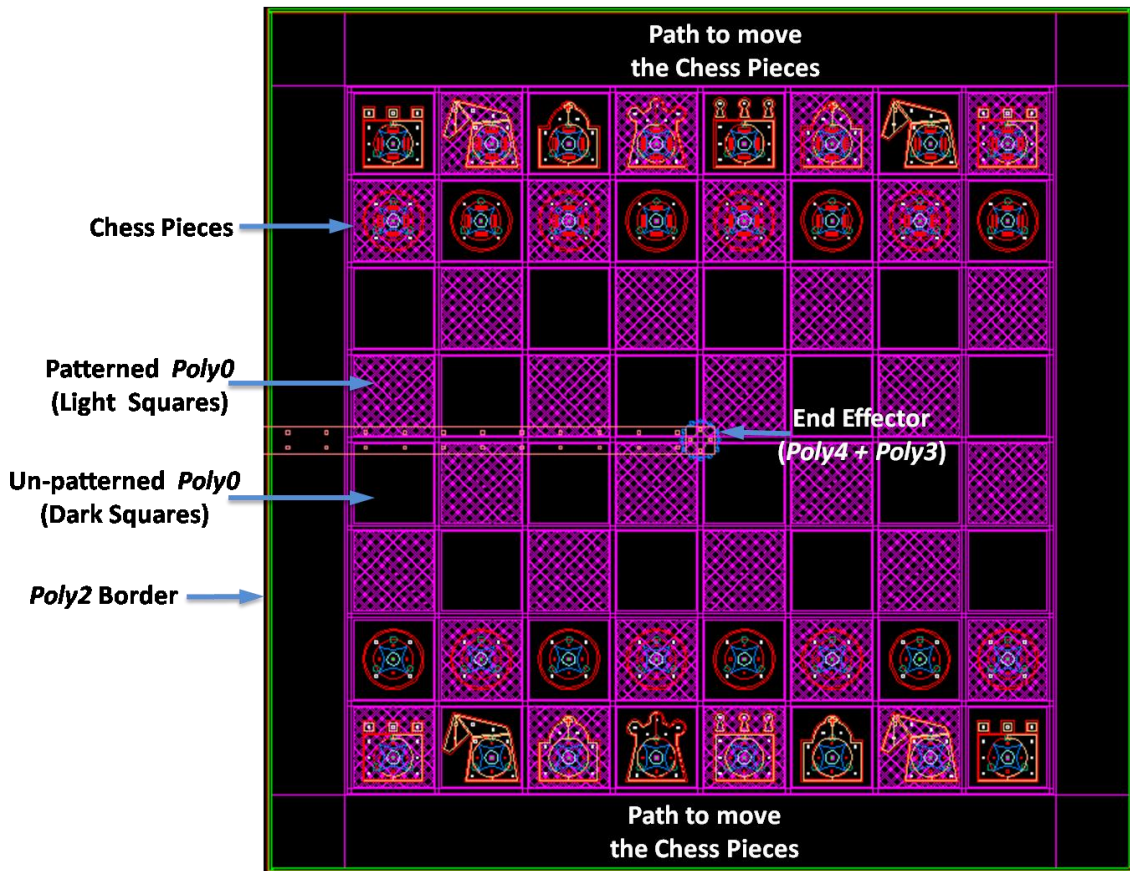


Figure 2: Layout of chess board and its key design components

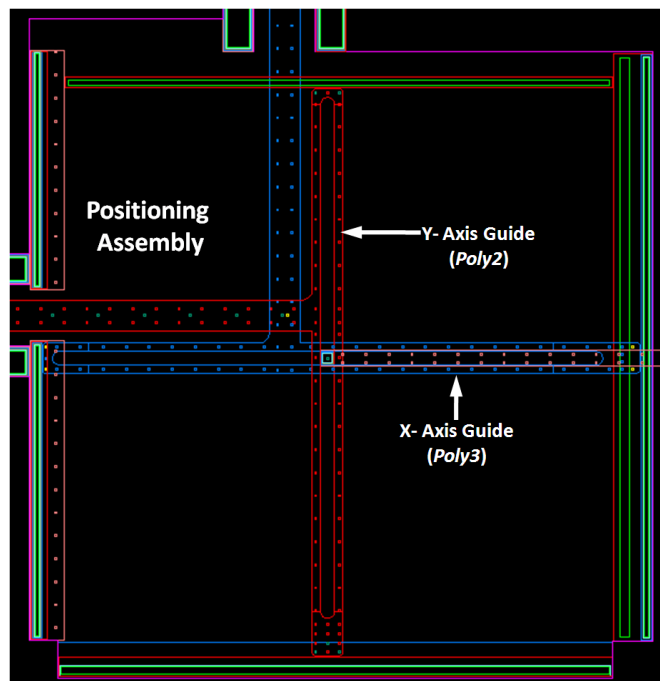


Figure 3: Positioning Assembly with slotted arms for movement along XY-axes

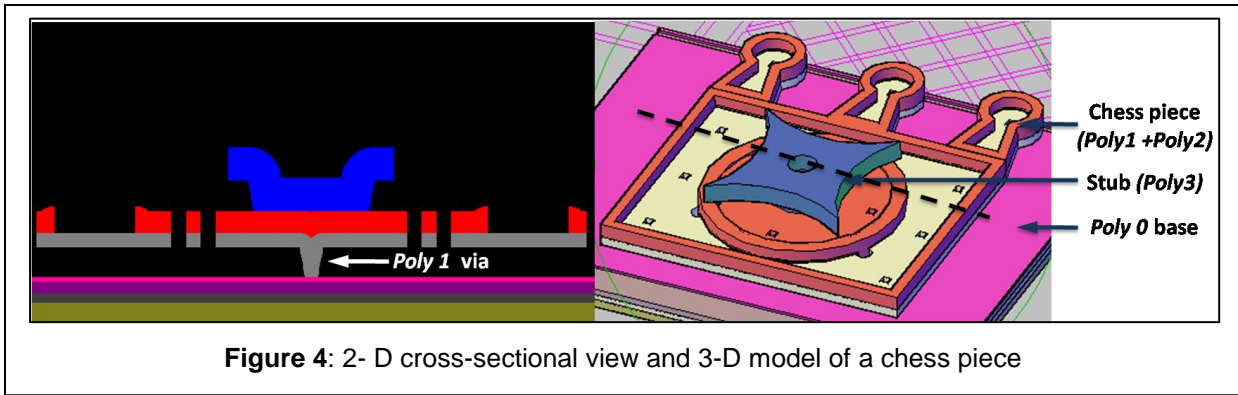


Figure 4: 2-D cross-sectional view and 3-D model of a chess piece

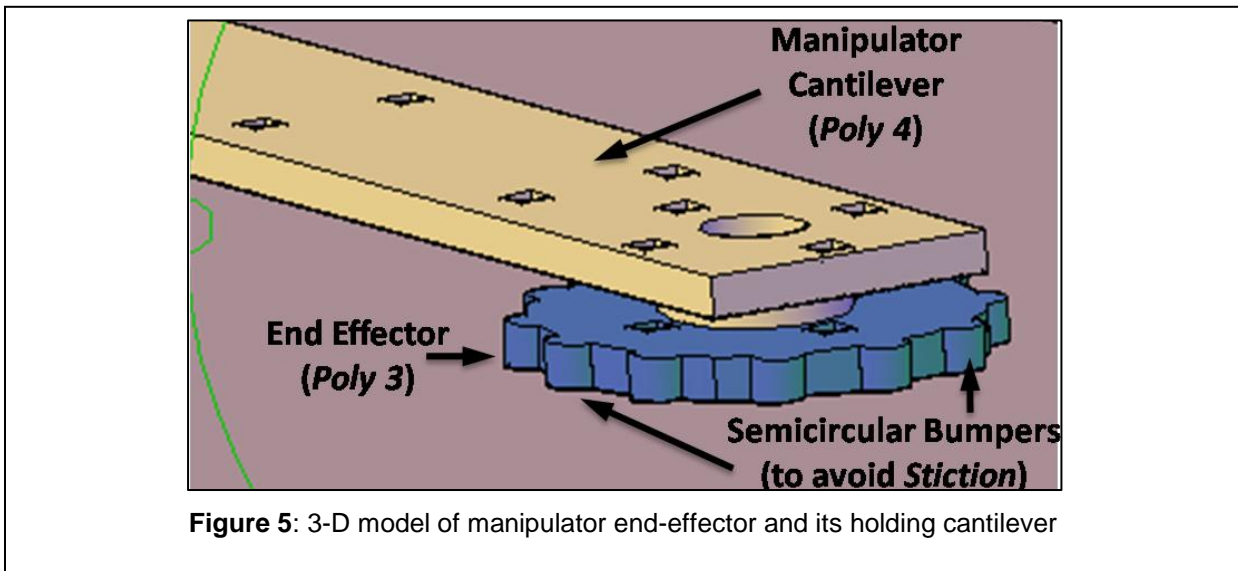


Figure 5: 3-D model of manipulator end-effector and its holding cantilever

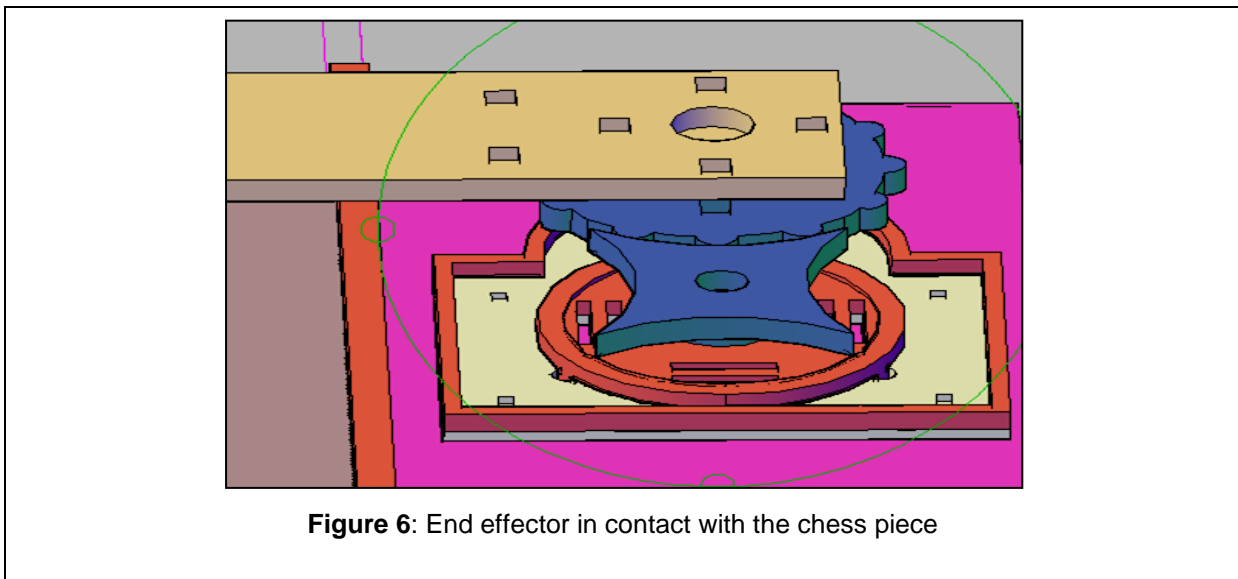


Figure 6: End effector in contact with the chess piece

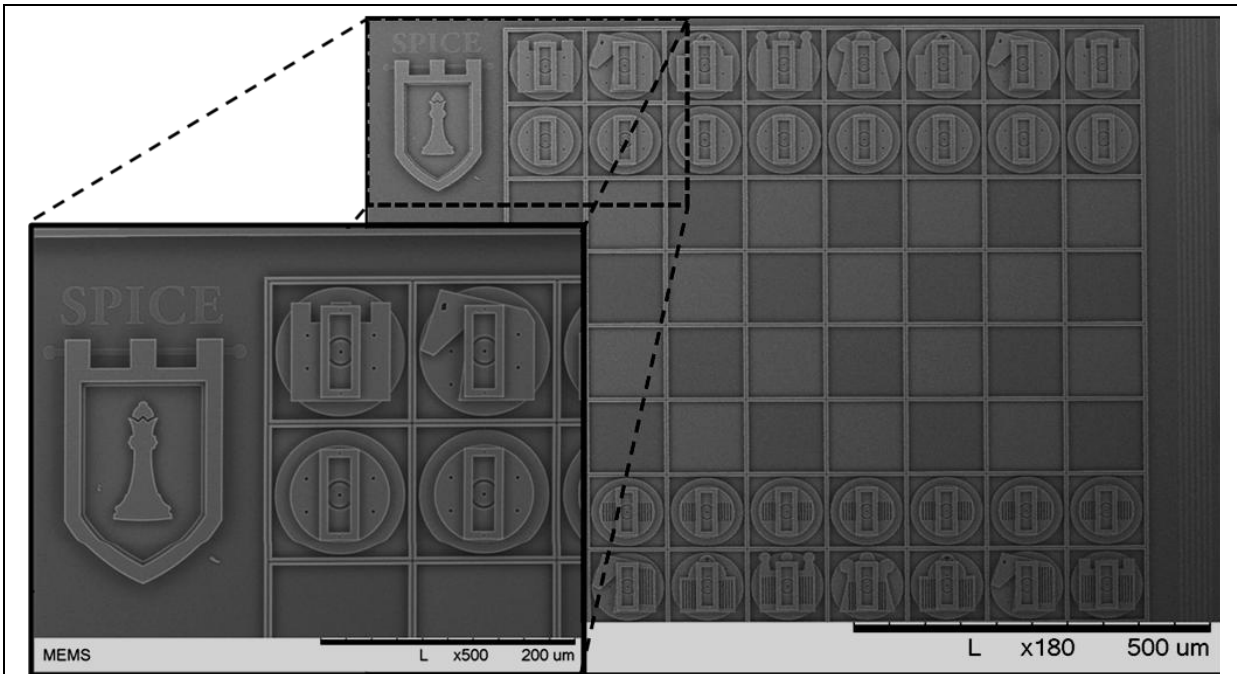
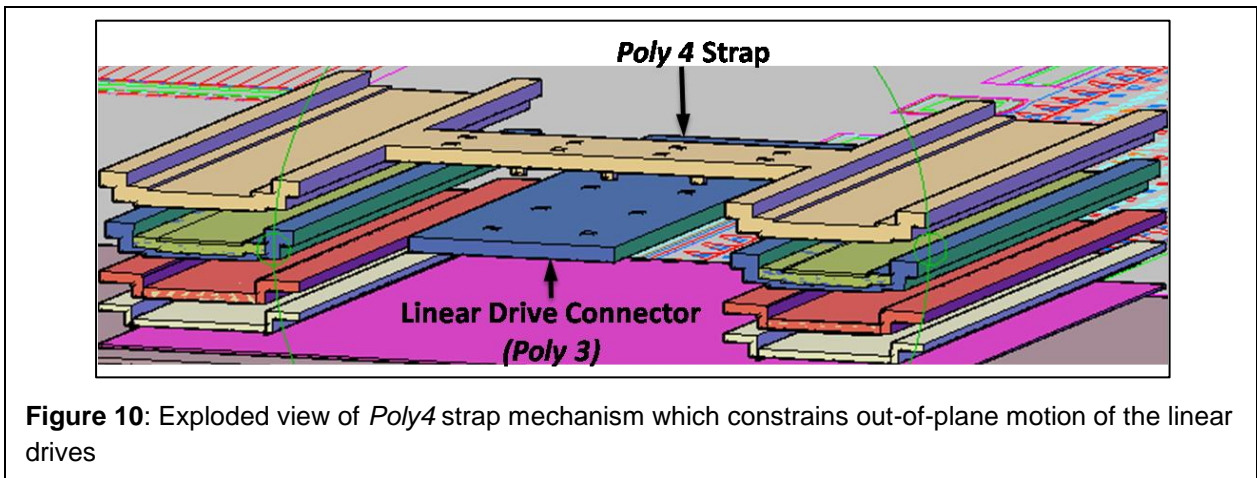
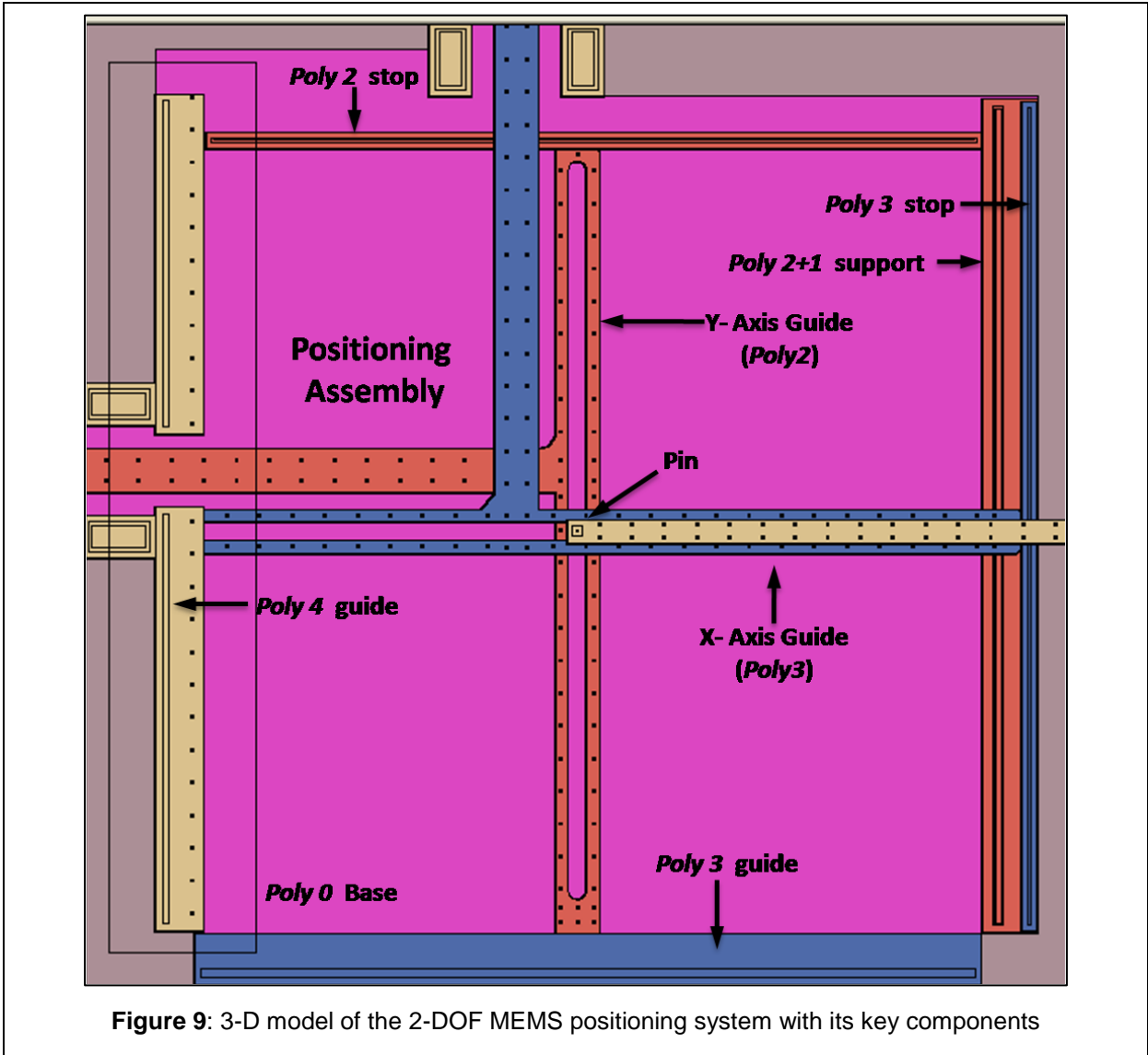


Figure 7: SEM pictures of previously fabricated Chess board at TTU. This design worked on the principle of 'Pick and Place'.



Figure 8: An off-chip metal micro-probe is used to manipulate a chess piece.



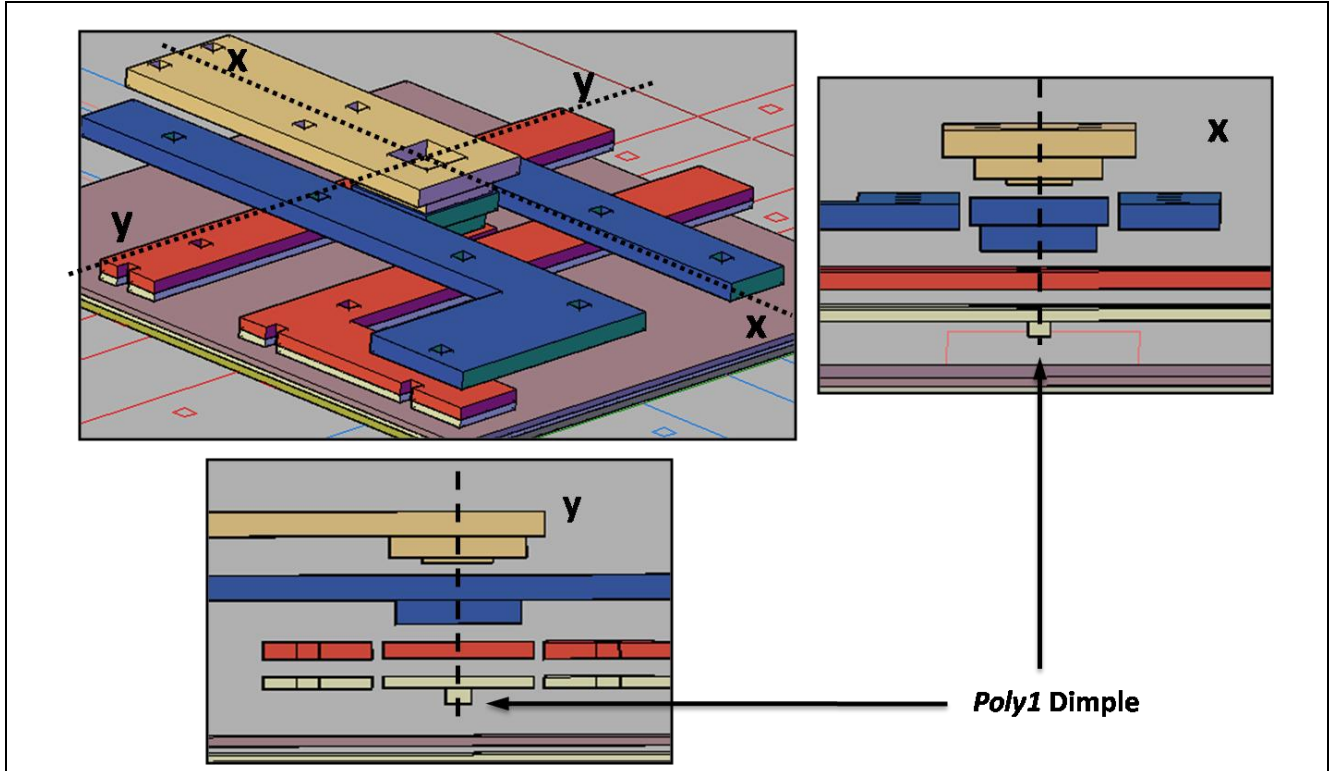


Figure 11: 3-D model image of the pin and track arrangement with dashed lines showing the exploded views.

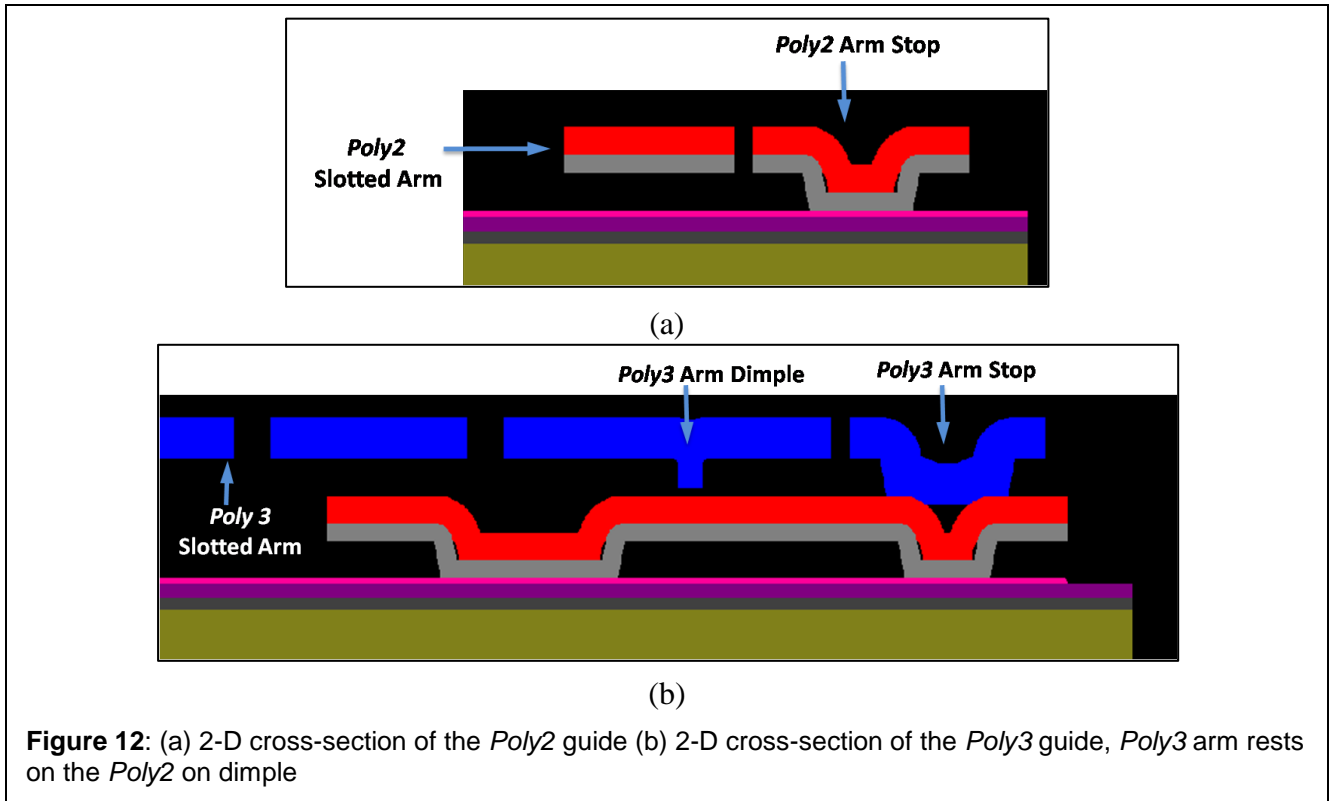
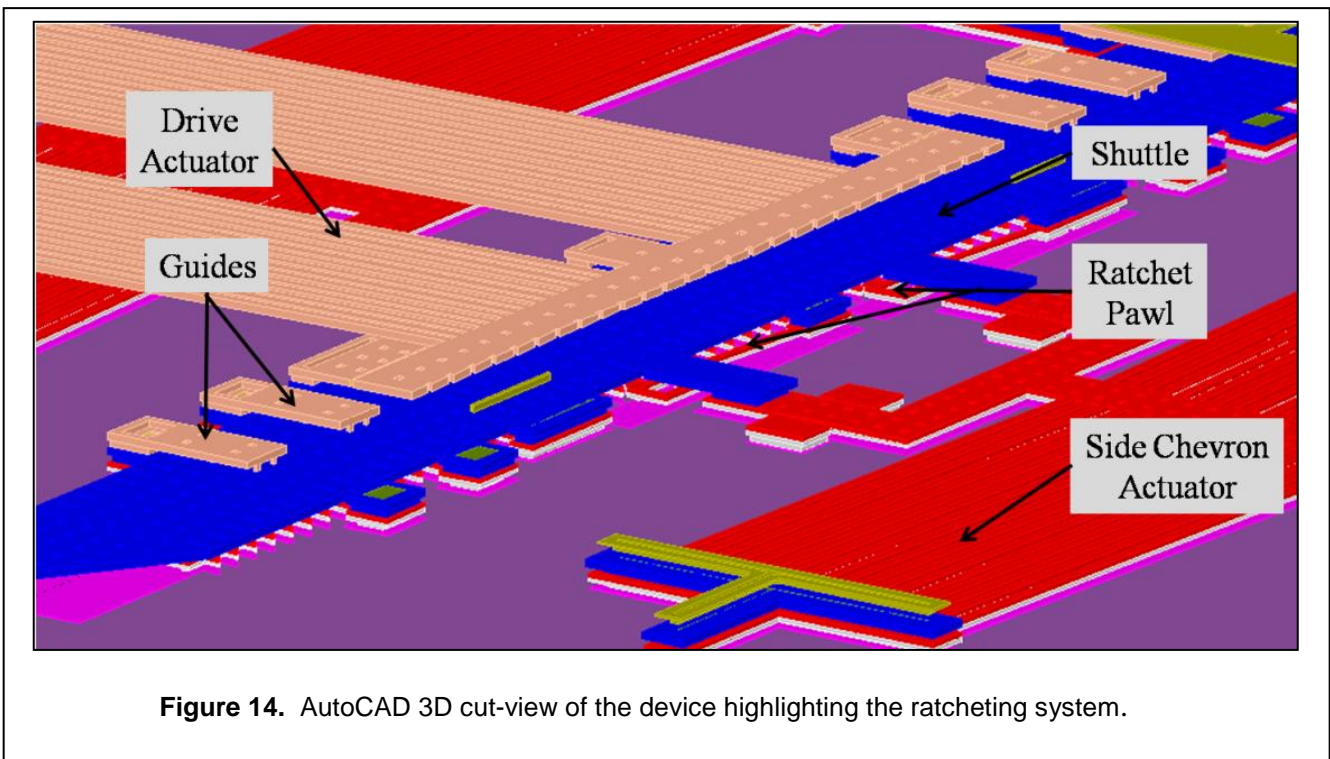
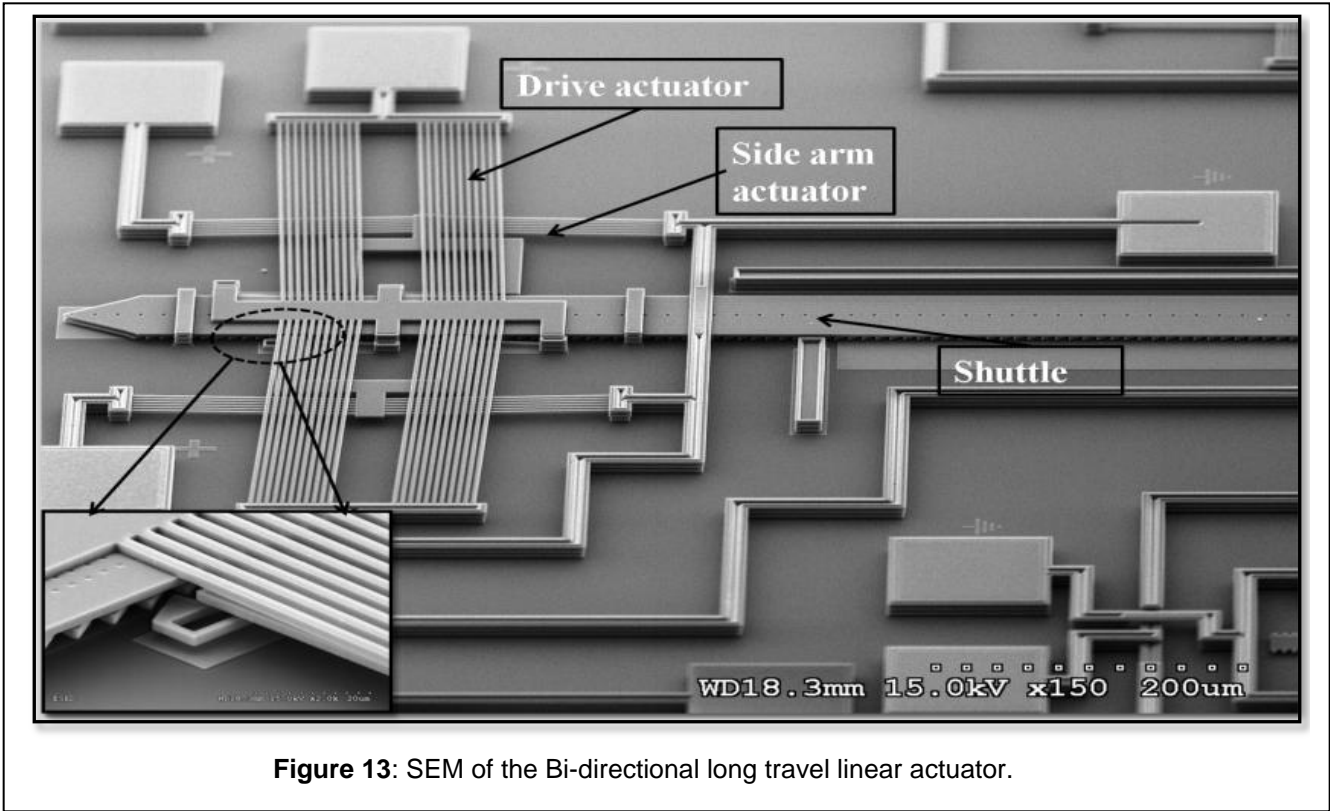


Figure 12: (a) 2-D cross-section of the Poly2 guide (b) 2-D cross-section of the Poly3 guide, Poly3 arm rests on the Poly2 on dimple



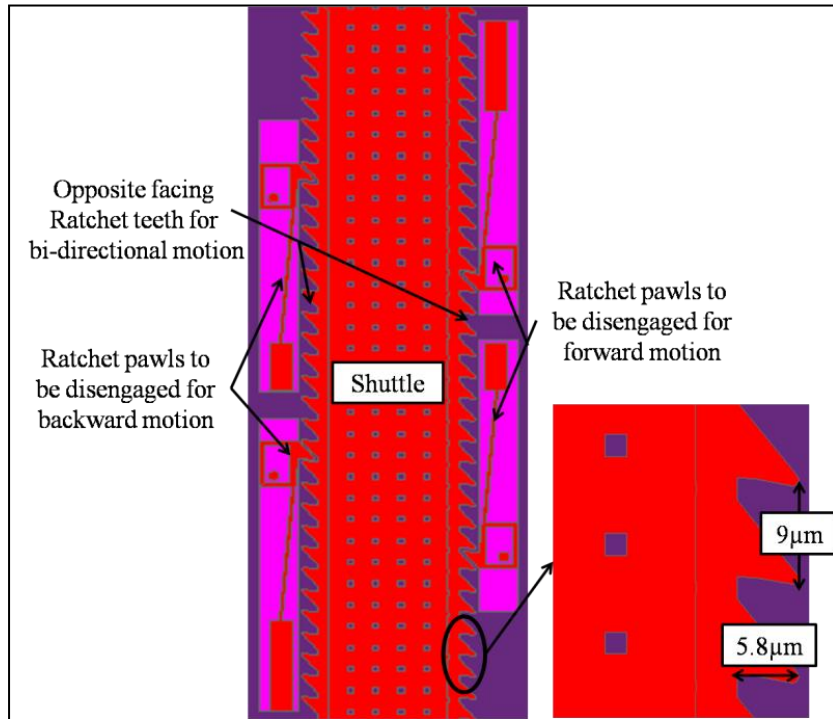


Figure 15: 3D model of the central shuttle with ratchet pawls, showing opposite facing serrated teeth along with their dimensions.

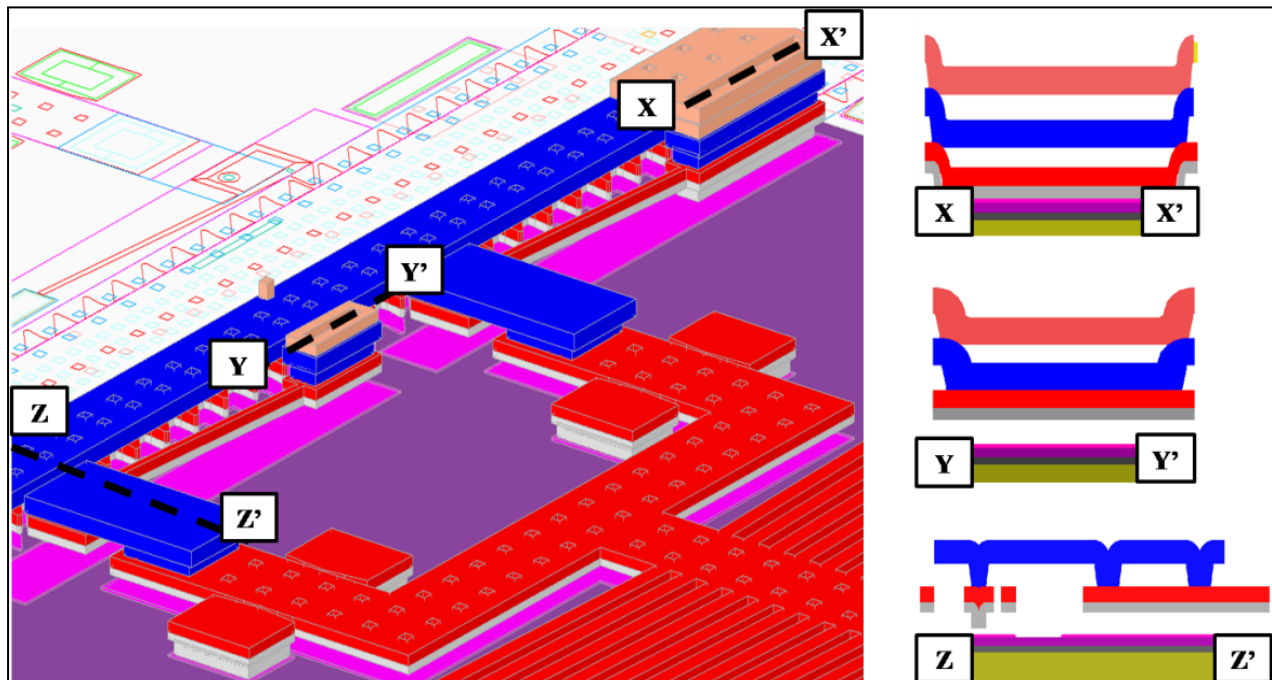
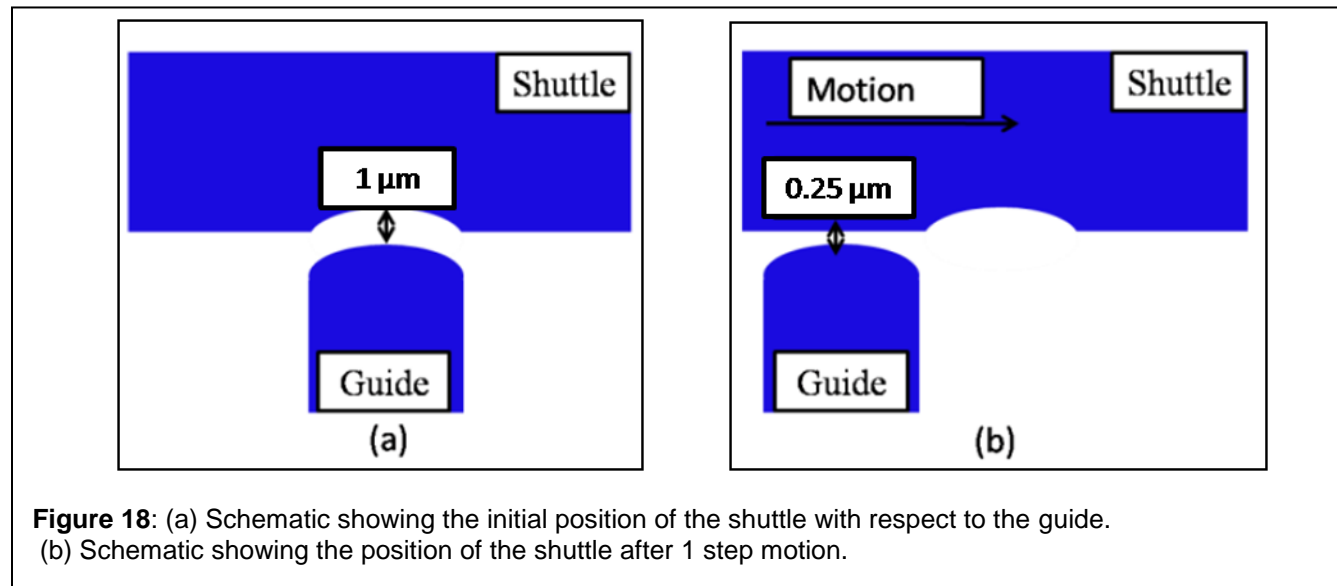
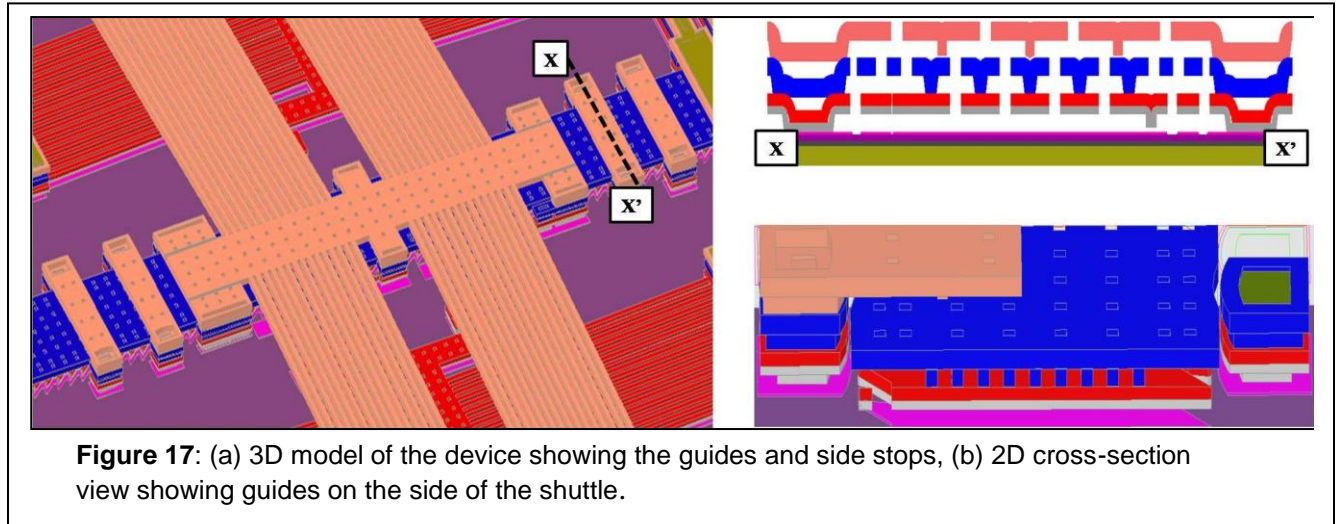
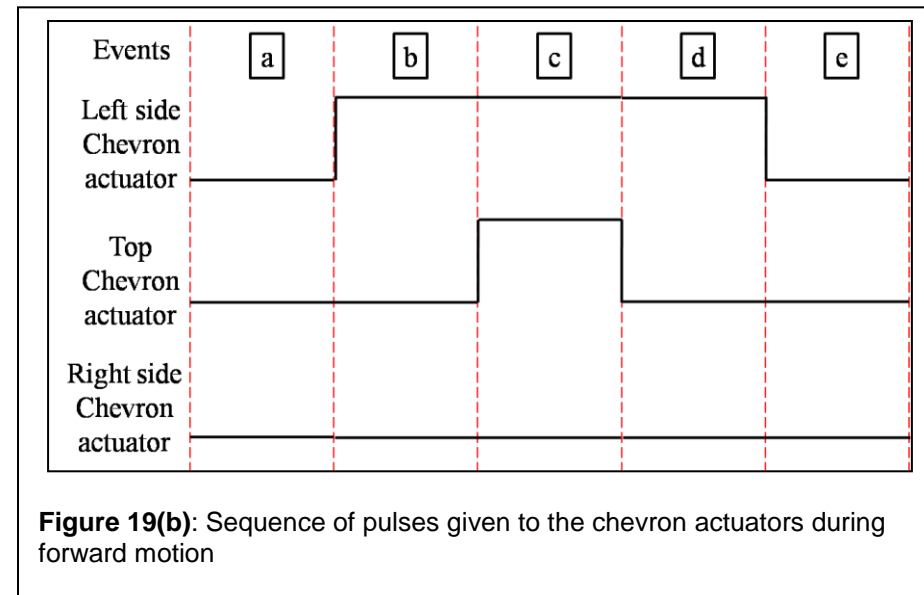
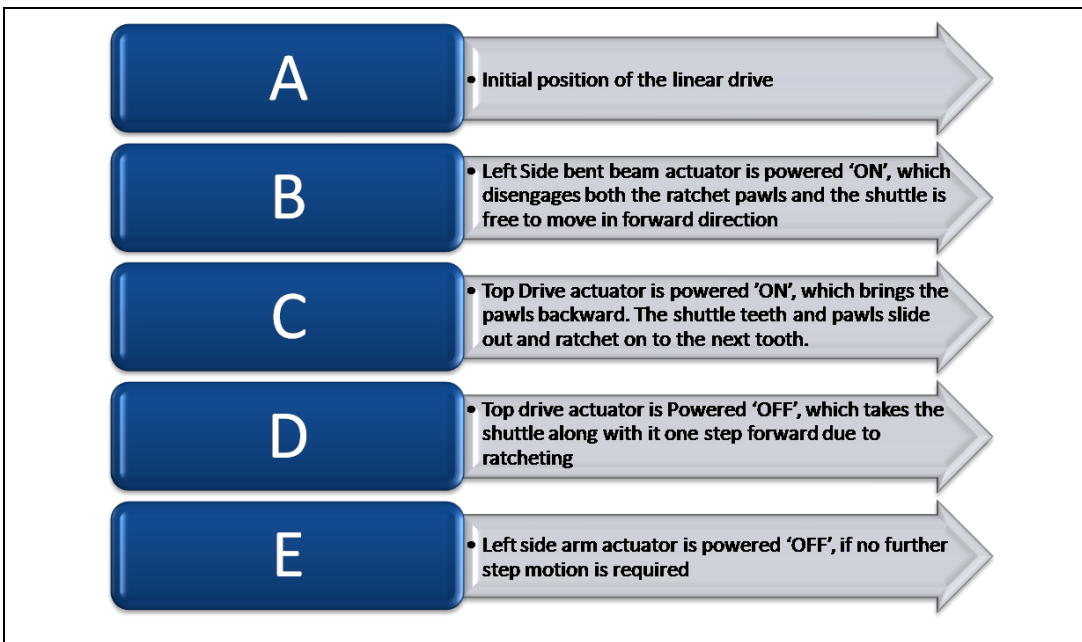
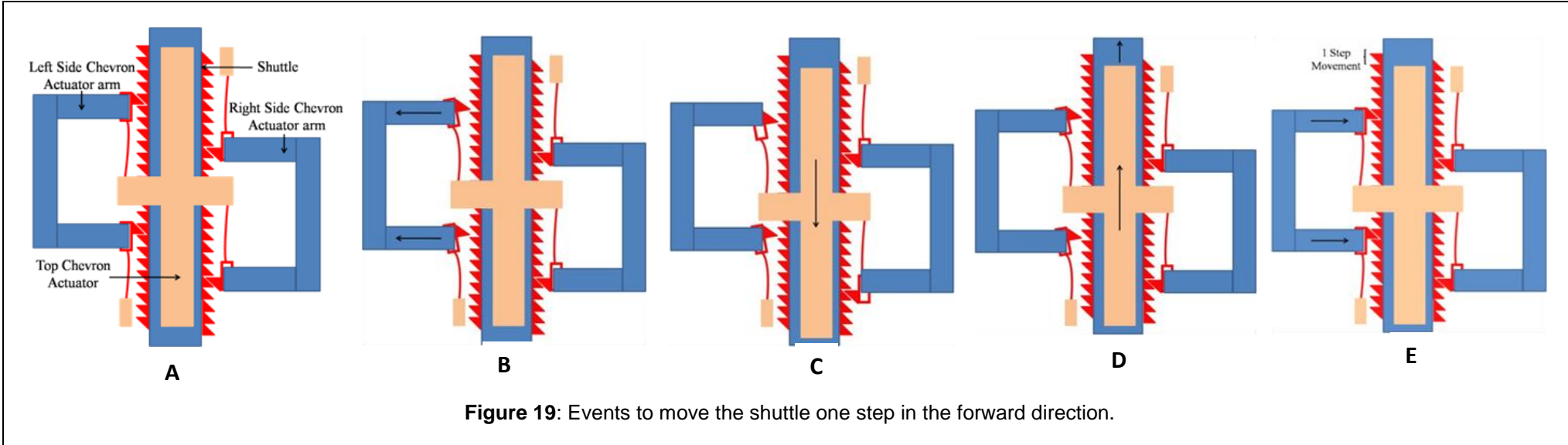
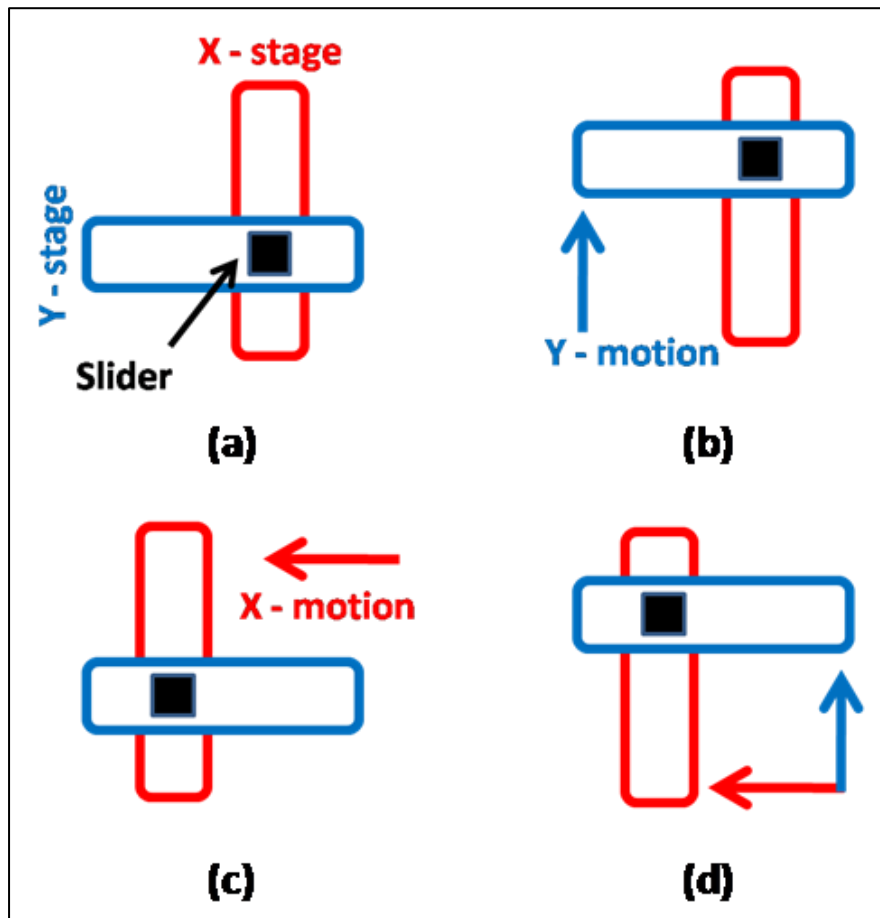


Figure 16: (a) 3D cut model of the device showing the two types of ratchet pawls and their coupling with the side chevron actuator, (b) 2D cross-section view of the anchored ratchet pawl, (c) 2D cross-section view showing the second ratchet pawl attached to the drive actuator, and (d) 2D cross-section view of the ratchet pawl coupled to the extended chevron arm.

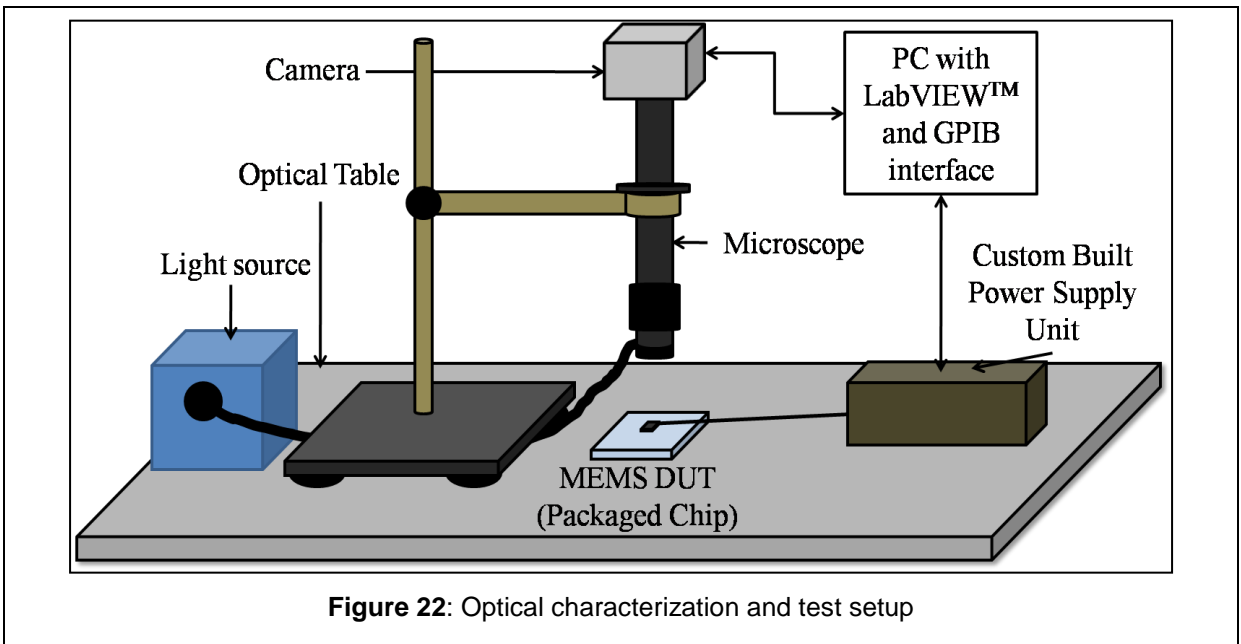
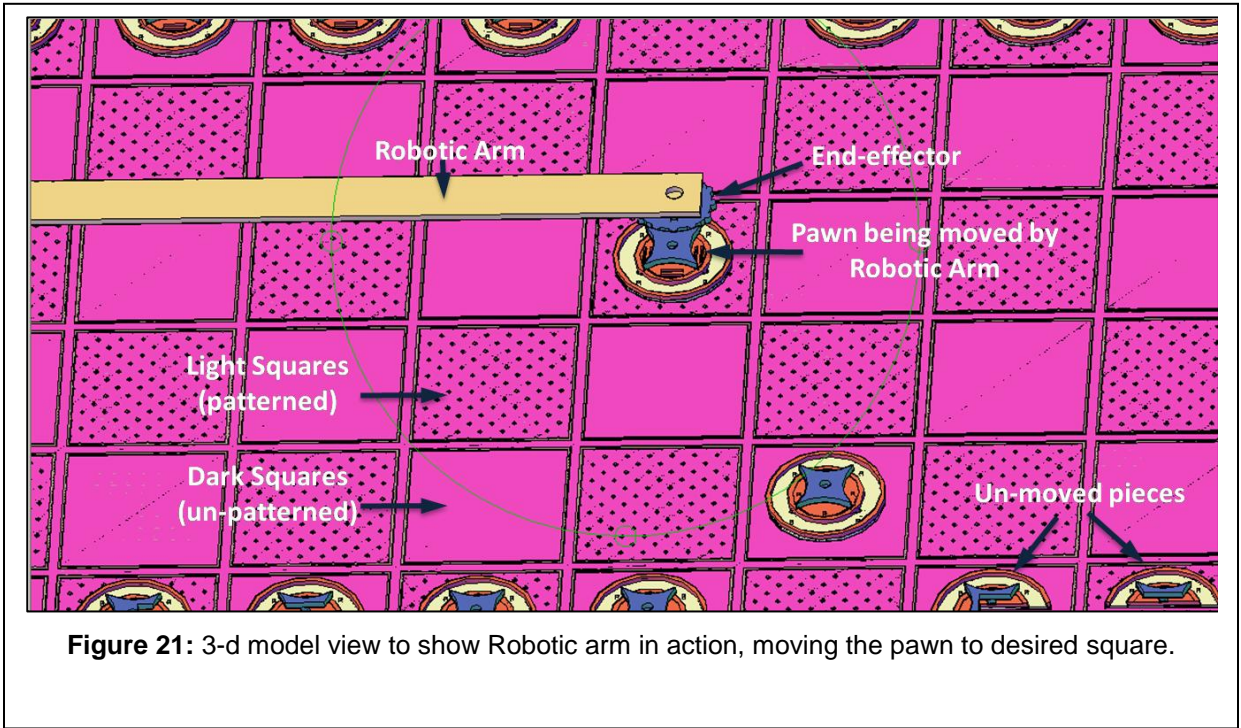


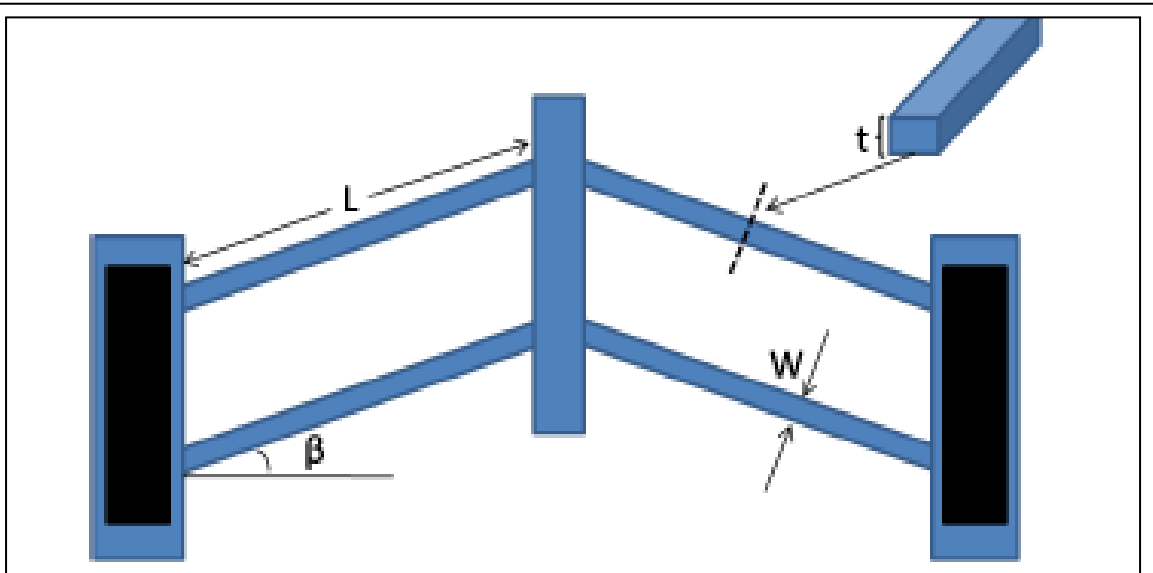




- a** • Top-down illustration showing main pin and slotted stage arms
- b** • To move in the Y-direction, a force to the right is applied to the vertical arm.
- c** • To move in the X-direction, a force is applied downward to the horizontal arm.
- d** • Concurrent motion along X-Y directions

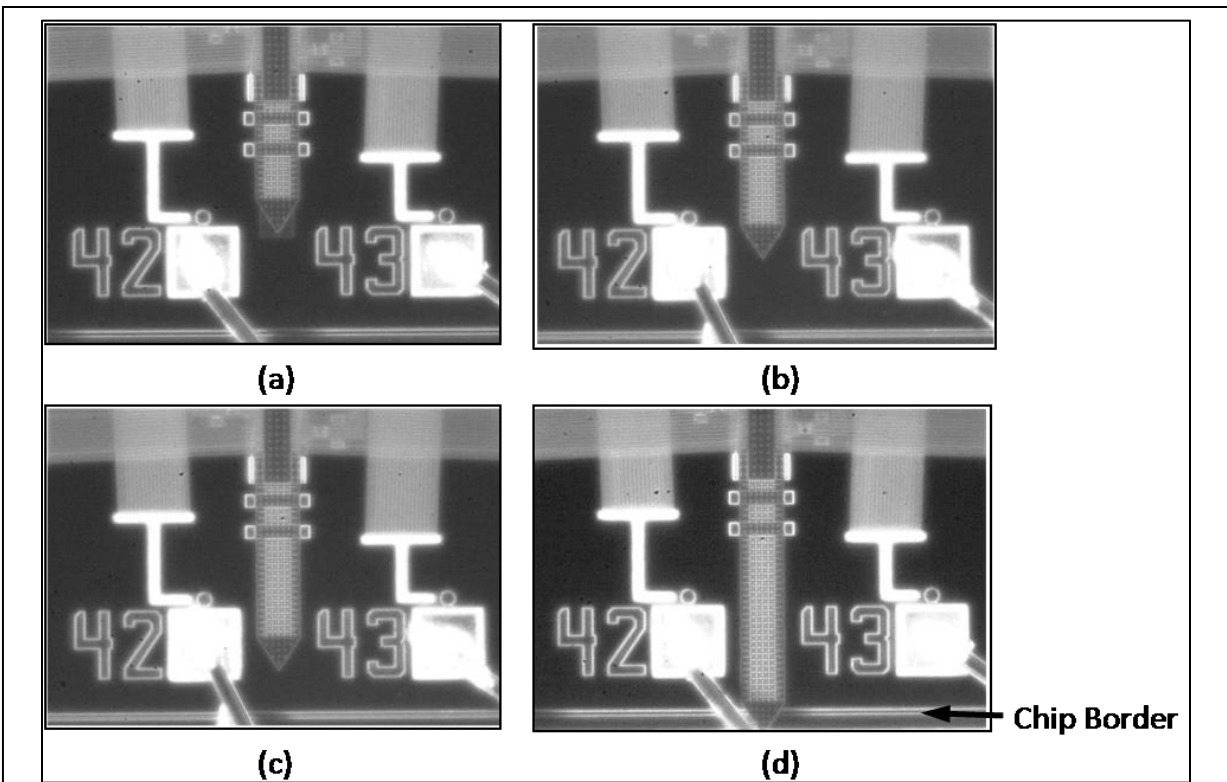
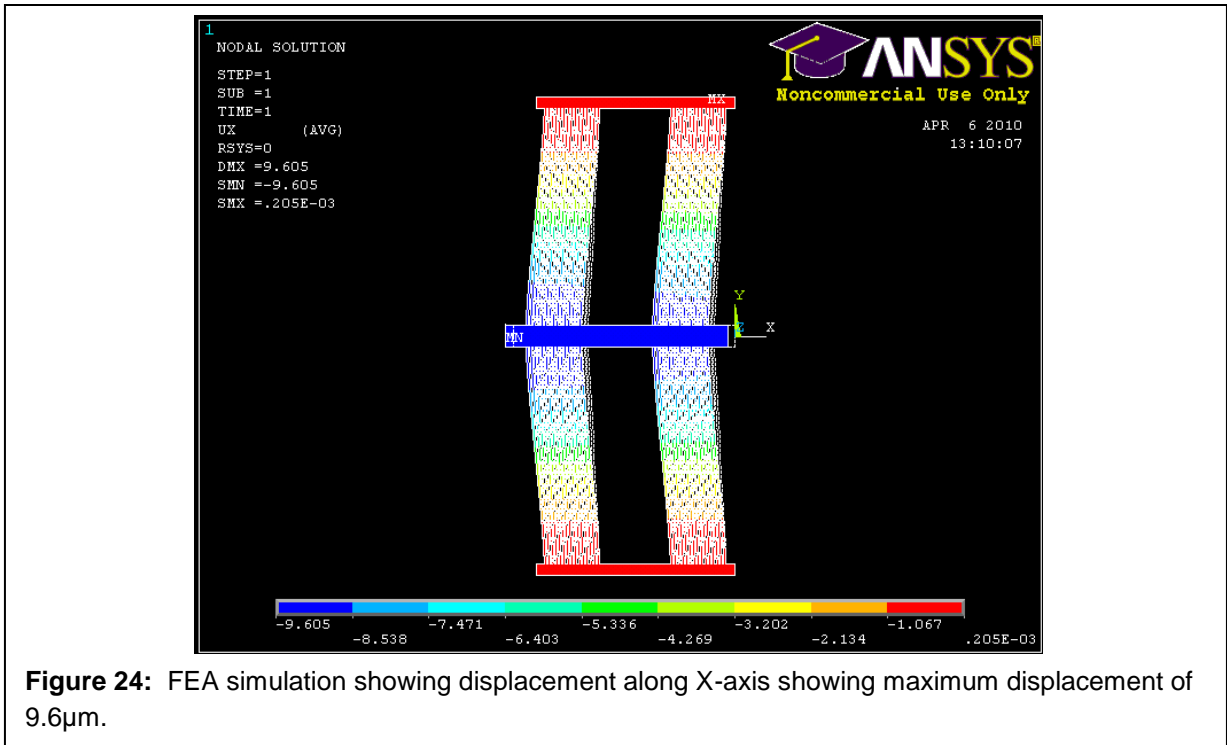
Figure 20: Illustration of the pin motion along X, Y and X-Y axis

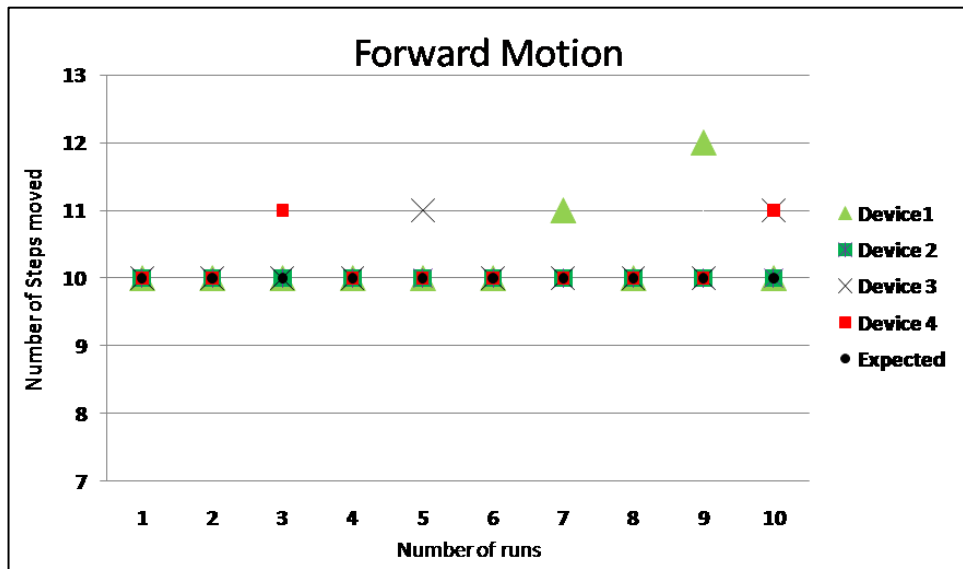




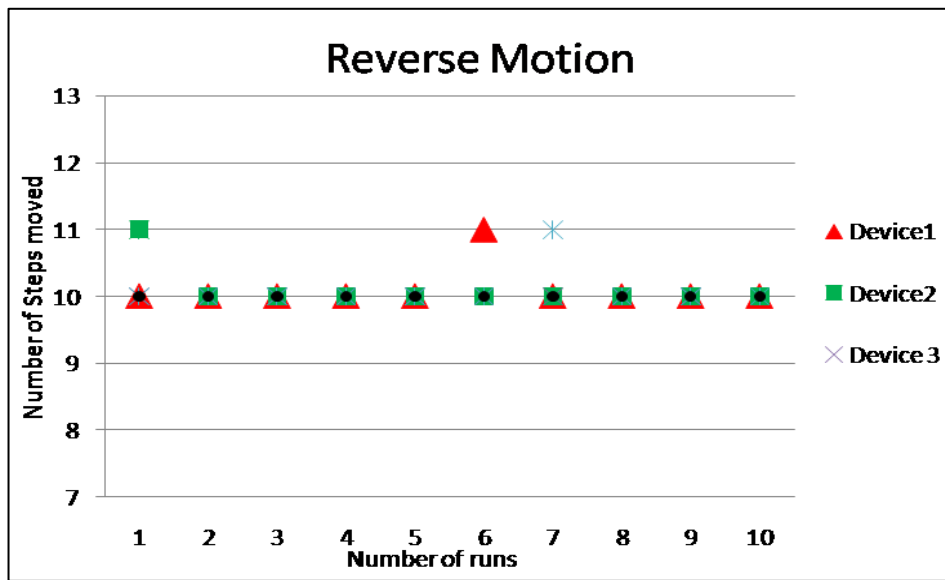
	Side Arm Actuator	Drive Actuator
Length of the beam (L)	200 μm	325 μm
Width of the beam (W)	3.5 μm	3.5 μm
Angle of the beam	2°	2°
Layer thickness (t)	2.5 μm	2.25 μm
Total number of beam	18	30
Function	Engage/ Disengage pawls	Drive the shuttle

Figure 23: Illustration showing dimensions for the bent beam actuators used in the design



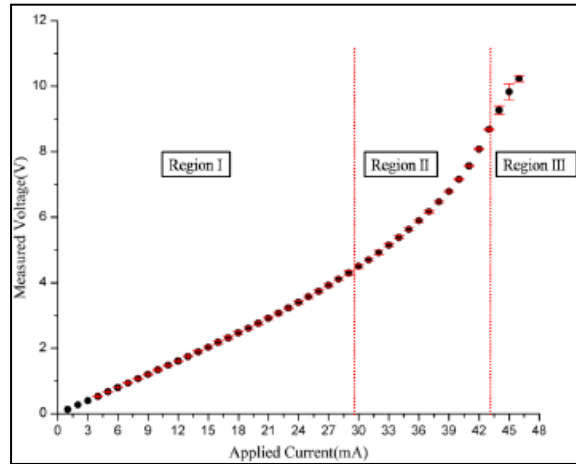


(a)

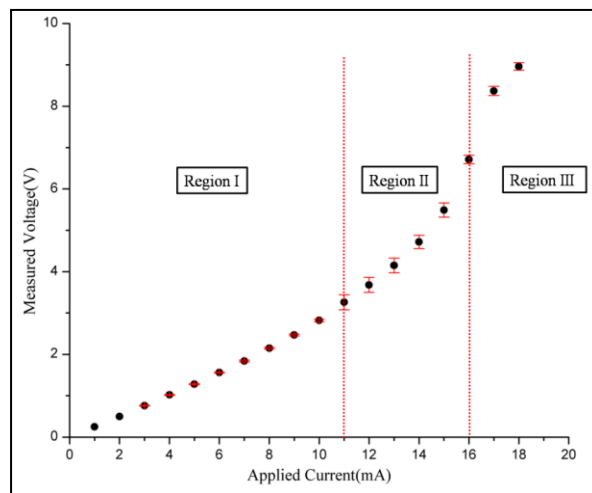


(b)

Figure 26: Plot of number of steps moved with respect to number of runs with each run constituting 10 actuation cycles, (a) Forward motion (b) Reverse motion.



(a)



(b)

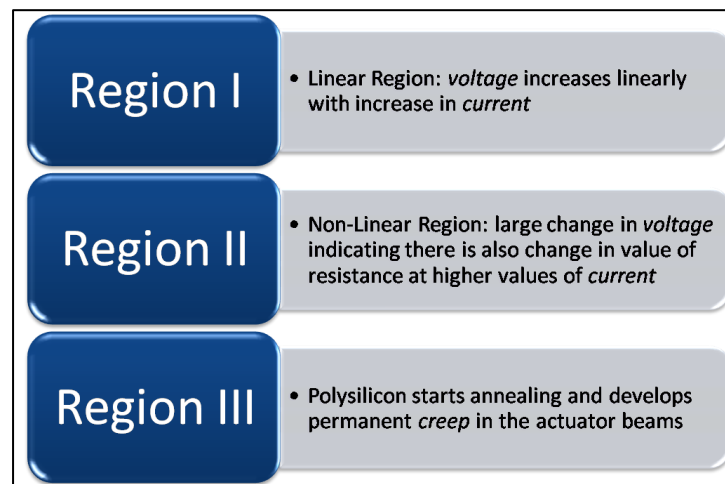
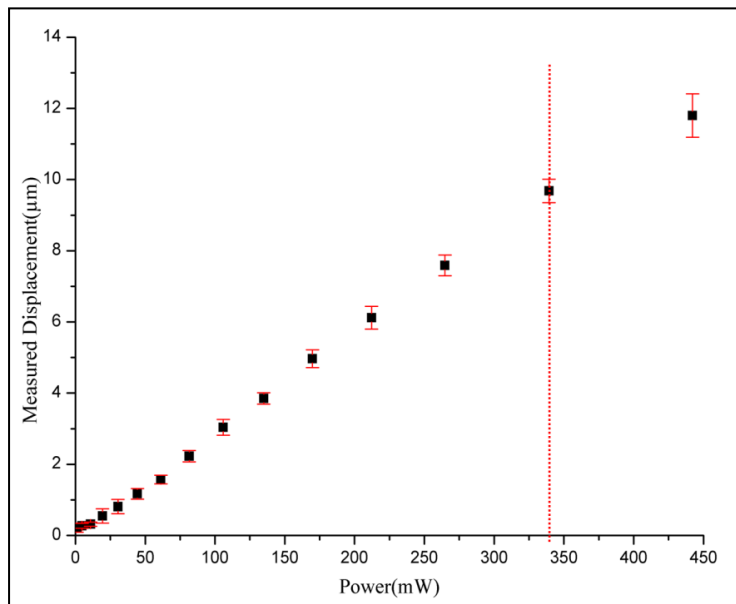
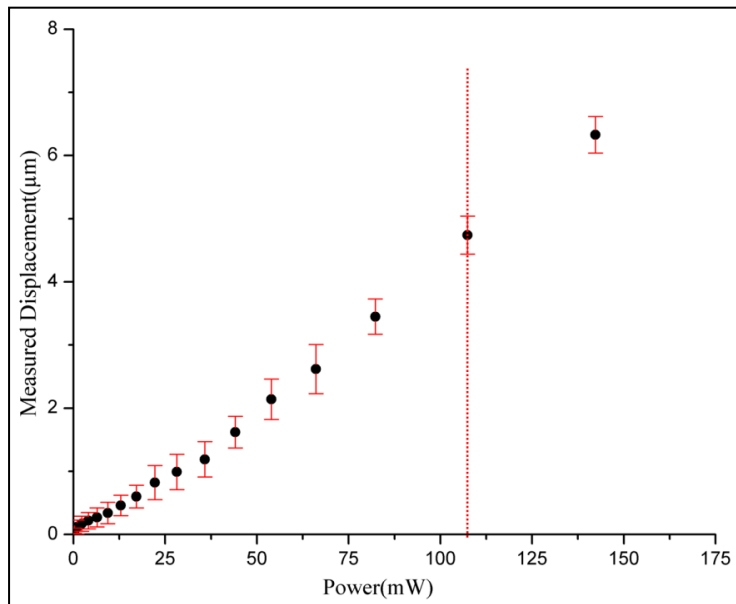


Figure 27. Plot of measured voltage with respect to applied current, (a) Drive actuator, (b) Side arm actuator.



(a)



(b)

Figure 28: Plot of measured displacement with respect to Power, (a) Drive actuator (330mW), (b) Side arm actuator (107mW)

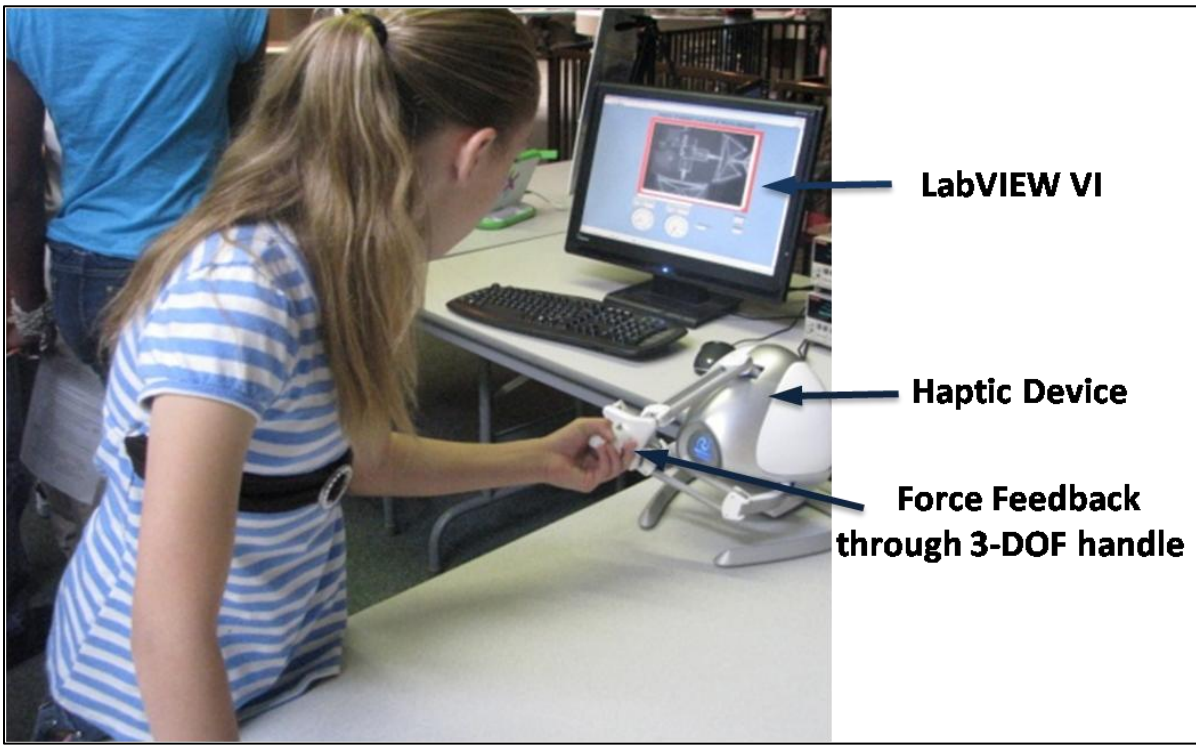


Figure 29: Elementary student actuating MEMS during Nano Day at Science Spectrum, Lubbock.

IX. Appendix B: References

- [1]Requicha A A G 2003 Nanorobots, NEMS, and nanoassembly *Proc. IEEE* **91** 1922–3.
- [2]Chen H P, Xi N and Li G Y 2006 CAD-guided automated nanoassembly using atomic force microscopy-based nonrobotics *IEEE Trans. Auto. Sci. Eng.* **3** 208–17
- [3]Sitti M and Hashimoto H 2000 Controlled pushing of nanoparticles: modeling and experiments *IEEE Trans. Mech.* **5** 199–211
- [4] Dong L X, Tao X Y, Zhang L, Zhang X B and Nelson B J Nanorobotic spot welding: controlled metal deposition with attogram precision from copper-filled carbon nanotubes *Nano Lett.* **7** 58–69.
- [5]Fukuda T, Arai F and Dong L 2003 Assembly of nanodevices with carbon nanotubes through nanorobotic manipulations *Proc. IEEE* **91** 1803–18
- [6] J. Muthuswamy *et al.*, "An array of microactuated microelectrodes for monitoring single-neuronal activity in rodents," *IEEE Transactions on Biomedical Engineering*, vol. 52, pp. 1470-1477, (2005).
- [7] Sandesh Rawool; Ganapathy Sivakumar; Johan Hendriske; Daniel Buscarello; Immanuel Purushothaman; Tim E. Dallas, "Development and testing of a multi-level chevron actuator based positioning system," in *SPIE Photonics west Proceedings* Vol. 7592.
- [8] *ANSYS User's Guide*, Release 10.0A1, ANSYS, Inc, 2006.
- [9] M. S. Baker, R. A. Plass, T. J. Headley, and J. A. Walraven, , "Compliant Thermo-mechanical MEMS Actuators," Sandia National Laboratories, Albuquerque, New Mexico, Tech. Rep. LDRD #52553, SAND2004-6635, Dec. 2004.